3D FEM and MBS Coupling of Railroad Dynamics with Vibration of Surrounding Building Structures

by

Chaitanya R Joshi
B.S. (University of Mumbai) 2013

Submitted as partial fulfillment of the requirements
for the degree of Master's of Science
in Mechanical Engineering in the Graduate College of the
University of Illinois at Chicago, 2016

Chicago, Illinois

Defense Committee:
Dr. Craig Foster, Chair
Dr. Ahmed Shabana, Advisor
Dr. Carmen Lilley

This thesis is dedicated to my family

ACKNOWLEDGMENTS

Firstly, I would like to thank my parents, for without their constant support and blessings I would not have been able to come the USA for pursuing my dream of Master's degree. I have been very fortunate to have come here and pursue my academic dream.

I would like to thank my adviser Dr. Craig Foster from CME department and my shadow adviser Dr. Ahmed Shabana. Their constant guidance and help inspired me to constantly work towards my goal and successfully complete the research I had taken as my thesis. I would also like to thank Dr.Carmen Lilley to be on my thesis committee.

I would also like to thank all my lab mates, especially Ahmed El-Ghandour. He constantly helped me throughout my research and without whose help I would have most certainly not been able to finish what I had started. Lastly, I would like thank all my friends for always being there through thick and thin.

TABLE OF CONTENTS

LIST OF TABLES

LIST OF FIGURES

LIST OF FIGURES (Continued)

FIGURE **PAGE**

LIST OF ABBREVIATIONS

FE	Finite Element
MBS	Multibody Systems
FFR	Floating Frame of Reference
ECF	Elastic Contact Formulation
ANCF	Absolute Nodal Coordinate Formulation
SAMS	Simulation of Articulated Mechanical Systems (a multibody software package)
MAPDL	Mechanical ANSYS Design Parametric Language

SUMMARY

With the advent of faster trains and changing railway technology, ensuring passenger safety and comfort has become an important area of research in the rail industry. The abatement of vibrations is also important and must be evaluated for new technologies. This research uses the coupling of finite element modeling and multibody dynamics to model a three-dimensional track system including rail, sleepers, ballast, substructure, and a nearby building. After conducting an initial modal analysis of the rail and sub-structure, we run a multibody simulation of a passing train to determine modal displacements and contact forces. We then reconstruct the full displacement field in a finite element software package and quantify the vibrations on the building. The ultimate goal is to quantify the vibrations in the building structure and understand the discomfort of the occupants.

Keywords: Finite element method, multibody dynamics, floating frame of reference, vibration analysis

CHAPTER 1

INTRODUCTION

This thesis examines building vibrations produced by passing trains using advanced computational modeling. The effect of train movement over rails causes the substructure, ground, and buildings surrounding the track to vibrate, which may cause occupant discomfort and, in extreme cases, building damage. With more advanced technology and faster trains, the amount of research on railroad dynamics concerning safety and comfort factors has increased. The rail substructure that transmits the vibrations begins with the sleepers, or crossties, which support the rail track and transmit loads to the ballast. The rail fasteners are also an important component of the track structure and help absorb the vibrations caused when the rail car moves over track. They act as a spring-damper system and maintain the connection between the rail and sleepers. The ballast forms a continuous base for the rail structure and supports it, as discussed in AREMA (1). The ballast is a gravel layer that absorbs the load and transfers it to the lower layers of the substructure, the subballast and subgrade. The subballast is a granular layer which transmits forces to the typically weaker subgrade, and helps prevent fine intrusion, frost heaves, and other undesirable behaviors. The subgrade is usually in situ soil, though it is often improved by compaction or other means.

With the enormous increases in computational power over past few decades, computer models have begun to play an increasingly important role in rail research. Computer models can greatly decrease the number of expensive tests needed to assess system safety, as well as

help understand the causes of observed issues in both controlled experiments and real accidents. A number of numerical studies have been performed to study rail behavior. Kumaran et al.(2) analyzed rail-wheel interaction of a moving train using finite element (FE) analysis. They studied the effect of passing trains on prestressed concrete sleepers. They modeled wheel-rail interaction and the entire rail-track structure to determine behavior of the sleepers. A number of other researchers have studied the rail-wheel interaction using finite element methods, including Sladowski and Sitarz (3), who simulated different rail and wheel profiles in order to examine the stresses on the components, particularly the rails. They specifically concentrated on the contact stresses from the rail-wheel interaction, examining the contact between the rail and wheel using different types of rail profiles. Monfared (4) examined the contact stresses on specifically the contact area during the rail-wheel interaction, while Li et al. (5) studied the vehicle-track interaction in underground railroad systems using finite element methods.

There have been few studies specifically in the area vibrations caused by trains, and their effects on nearby structures. Bednarz and Targosz (6) created a finite element model in one study to predict the magnitudes of vibrations in nearby buildings. They studied the wave propagation through ground and its effects on the surrounding structures. The FE model they used in their research consisted of tracks, sleepers, and substructure. A small part of the building was also modeled near the rail tracks. They concluded that the particular structure would experience accelerations greater than 0.005g, which by code would indicate potential occupant discomfort. Verbraken et al. (7) used an empirical formulation, verified with a finite element model, to predict vibration velocities in buildings. They found that under some

circumstances, the model required appropriate force density measurements for accurate results. This force density can be determined nuermically (e.g. through a finite element model) or experimentally. They also explored some mitigation techniques.

In recent times, the field of multibody systems (MBS) dynamics has improved to the point where many sophisticated problems in mechanics can be solved. MBS is the study of the differential and algebraic equations used to model the mechanics of interconnected rigid and deformable bodies. The field is ideally suited to investigating mechanical problems in train dynamics, or the interaction of a train wheel with a rail. Multibody dynamics codes can be used to understand the deformations of the rail as well as estimate the contact forces between the wheel and rail. The study performed by Kumaran et al. (2) discusses various methods to understand the dynamics of the rail-wheel interaction. MBS has been used to model the moving trains, including rail-wheel contact, as discussed in Shabana et al. (8) and Recuero et al. (9). Recuero et al.(9) studied the effects of unsupported sleepers on the rail track system using non-linear multibody dynamics approach, showing higher forces induced by lack of support in one area. Coupling finite element and multibody analysis has become a useful approach for investigating rail-wheel interaction. Dynamic rail-wheel interaction was studied by Tanabe et al. (10) using a coupled FE and MBS model. They studied the interaction under earthquake conditions on a high speed train during a derailment during an earthquake type situation. Galvin et al. (11) discussed the rail-wheel interaction in high speed trains. They used a finite element approach and created a model studying the train-track-soil interaction and studied the effects of vibrations in near by structures. El-Ghandour et al. (12) use a coupled model

to investigate the effect of the substructure on track stiffness. They used a floating frame of reference technique to understand the effect of the substructure on rail-wheel interaction.

In this research, we couple a finite element model of the track substructure with a multibody dynamics code that can more accurately capture the wheel-rail interaction and hence more accurately predict the forces which drive substructure deformation. The finite element model was created in the commercially available FE software ANSYS using the Mechanical ANSYS Parametric Design Language (MAPDL), and includes the properties and geometry of the rail, fasteners, sleepers, and track substructure, as well as modeling a building near the track. A modal decomposition is performed for efficiency, and the modal mass and stiffness properties are exported and then imported into the multibody code SAMS/rail. This code simulates the dynamic motion of the wheel over the track, including a sophisticated wheel-rail contact algorithm. The formulation we used in the MBS code is the floating frame of reference technique. The floating frame of reference technique, as explained by Shabana et al. (8), is a method to analyze the dynamics of any multibody system undergoing small strains but large relative rotations. Other methods included in his paper are absolute nodal coordinate formulation (ANCF.)In this thesis, we model a single suspended wheelset passing over the track structure. The study uses the techniques from El-Ghandour et al. (12), but augments them to reconstruct the full nodal displacements of the model from the modal displacements. Once these are known, the displacements, strains, accelerations, and other quantities can be determined in the system.

The remainder of the thesis is structured as follows: Chapter 2 outlines the finite element model of the track and substructure. Chapter 3 Discusses the multibody dynamics analysis of

the system. The reconstruction of the full model in the finite element software is presented in Chapter 4. A numerical example is analyzed and discussed in Chapter 5. Finally, conclusions and future work are given in Chapter 6.

CHAPTER 2

FINITE ELEMENT MODEL

The Finite Element Method is one of the most versatile and popular techniques to model the mechanical, thermal, or other engineering behavior of a system, structure or a machine component. The method can handle complex geometries, material properties, and boundary conditions and analyze the response under loading to produce accurate results to many problems.

For this research, we build a three-dimensional model of the rails, fasteners, and sleepers, along with the track substructure, which includes ballast, subballast, and subgrade. We use the commercial finite code ANSYS to create the geometry and assign material and section properties.

The sleepers and rails are modeled with three-dimensional beam elements (BEAM4). The fasteners are modeled with spring-damper elements (COMBIN14). This relaxes the rigidity of the deformation between the rails and sleepers, capturing the combined effect of the fasteners and the rail pads.

The ballast, subballast, subgrade, and building were modeled using an 8-node hexahedral, or brick, element, SOLID185. While 20-node bricks have a higher order of interpolation, they are generally not preferred for dynamic applications, where the optimum mass matrix is difficult to identify. Each material modeled by the bricks is assigned its own unique material properties.

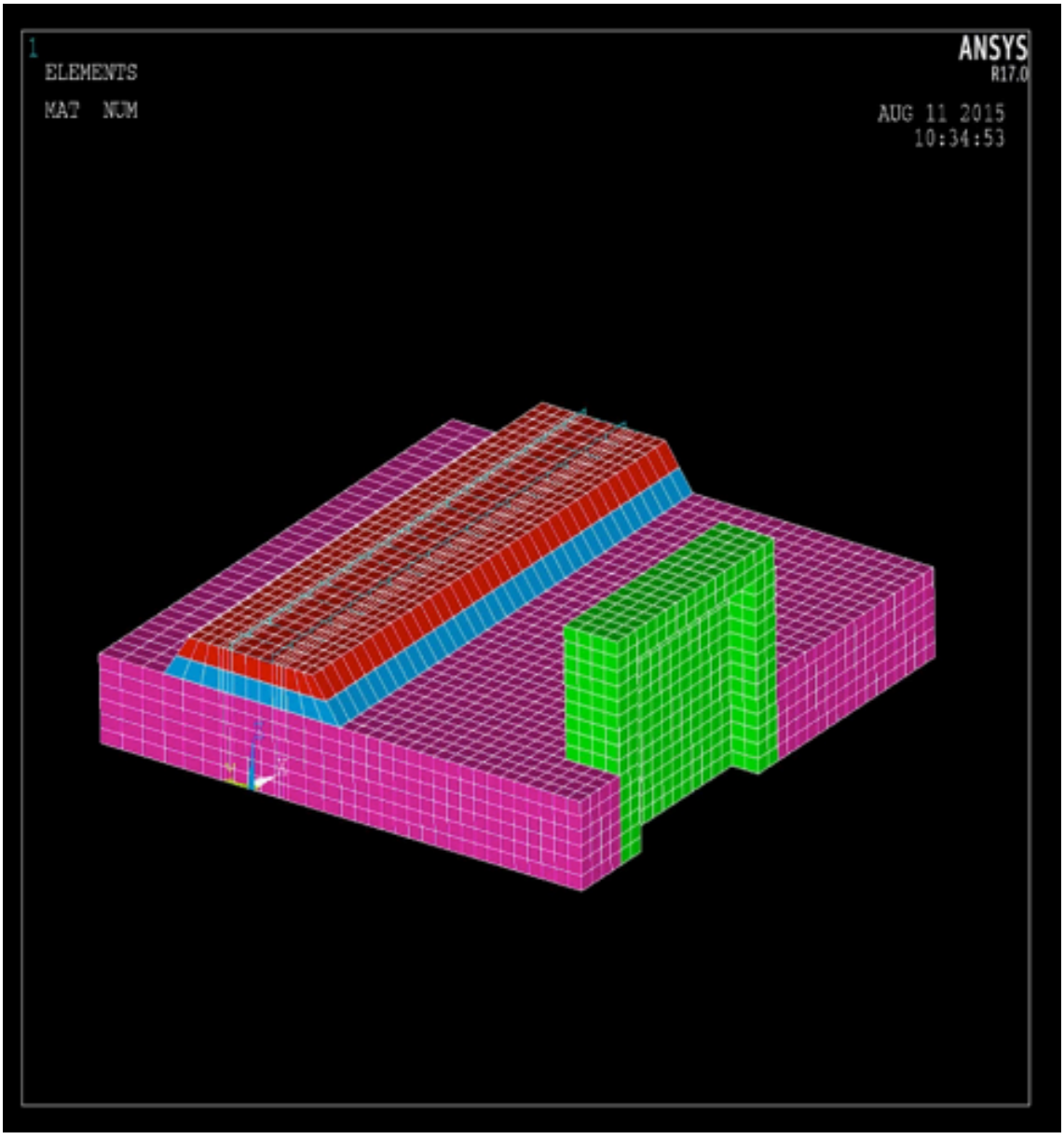

Figure 1. 3D finite element model of the rail track structure. Rails, sleepers, and fasteners are blue line elements. Ballast is red, subballast blue, and subgrade purple with the building in green.

The geometry is shown in Figure 1. Here the layers of the different materials are clearly visible. The model allows waves to travel from the rail through the substructure to the building, to measure vibrations. The bottom and sides are constrained for zero out-of-plane motion. The model is constructured entirely on ANSYS MAPDL (Mechanical ANSYS Parametric Design Language).

The material parameters for the finite element were taken from El-Ghandour et al. (12) with some modifications. The material properties of the railroad were specifically selected as per AREMA (1) standards. The full list of material parameters and section properties for the beam elements are discussed in Chapter 5 shown in Table I. Since we will perform a modal analysis, only linear properties of all the materials are considered here.

2.1 Modal analysis

Modal analysis is used to greatly reduce the number of degrees of freedom of a system and hence improve the efficiency of a simulation. It also reveals fundamental frequencies that, if excited, can cause strong motion in a structure and damage it. After creating the model of the three-dimensional railroad structure in the finite element software, we perform a modal analysis to obtain the eigenvalues and mode shapes of the structure. The modal mass and stiffness values are used to simulate the dynamic analysis of the rail-wheel interaction. After determining the mode shapes, we can eliminate the degrees of freedom in the shape vector that are not directly used in the multibody simulation. In this case, we retain only the degrees of freedom of rail, further improving the efficiency and greatly reducing memory requirements.

The modal analysis has been done on the commercially available with Block-Lanczos method. One of the mode shapes are shown in Figure 2.

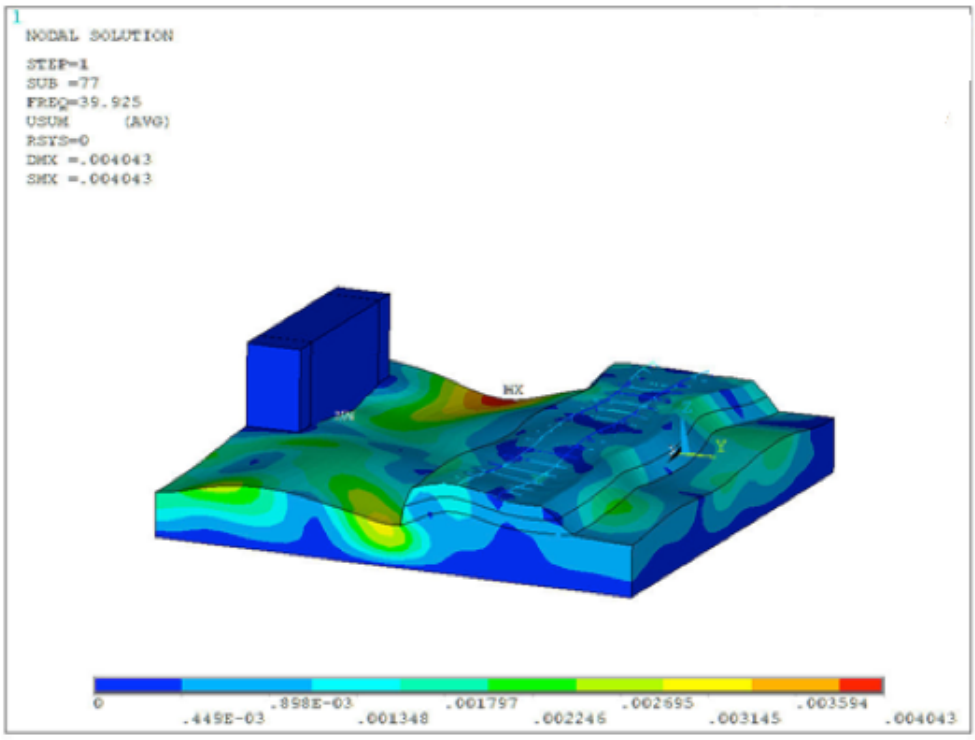

Figure 2. One of the fundamental mode shapes of the model.

El Ghandour et al. (12) demonstrated that a relatively large number of modes are necessary for an accurate solution for the rail problem, compared to many other problems. The reason for this need is the concentrated and moving nature of the load. Concentrated loads require a relatively large number of mode shapes to resolve the displacement, and even more are required

when the location of the load changes. The higher the number of modes, the more accurate the results are, especially for more complex geometries. Based on the study in (12), one hundred and twenty mode shapes were extracted from the model along with their mass and stiffness values. This information was used in the multibody code to create an efficient and relatively accurate model of the mass and stiffness of the track and substructure, as will be discussed later.

2.2 PreSAMS

In order to simulate our rail problem in the multibody dynamics code, we need to format the information from the finite element software for efficient input into the. The output data from ANSYS was read by the preprocessing program PreSAMS, which in turn produced input file for the multibody dynamics simulation. In PreSAMS, we truncate the mode shapes to include only the degrees of freedom that are used directly involved in the multibody simulation. Here, those are the degrees of freedom of the rail. We also adjust the format of the modal mass and stiffness to fit input file format for SAMS (Simulation of Articulated Mechanical Systems).

CHAPTER 3

MULTIBODY DYNAMICS MODEL

After performing modal analysis in the finite element software, we input the modal information into a multibody code to analyze the wheel-rail interaction over this flexible substructure. Multibody dynamics is a branch of computational mechanics studying the interaction of connected rigid and flexible bodies. In our research, we use the floating frame of reference for formulating the deformation of the bodies. This technique was used by Recuero et al. (9) and El-Ghandour et al. (12) in their investigation of rail performance.

The floating frame of reference (FFR), as discussed by Vlasenko and Kasper (13), determines the relative motion of the system of the elastic coordinates with respect to the reference coordinates, shown schematically in Figure 3. This formulation is appropriate for small deformations but can handle large relative rotations. For large deformations, this formulation can introduce error into the system, and an alternative approach such as the Absolute Nodal Coordinate Formulation (ANCF) can be used (14). For the problems under consideration, however, deformations are small and the more efficient FFR formulation is preferable. In the Floating Frame of Reference, the elements are considered as the part of a rigid and flexible body system. The motion of the component is defined with respect to the absolute fixed frame of reference. The position of point on the rail can be defined by

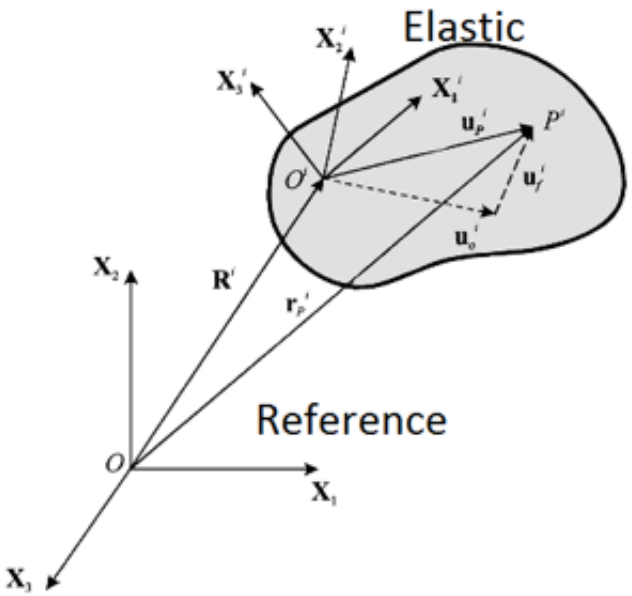

Figure 3. Representation of a body undergoing deformation

$$\boldsymbol{r}^i = \boldsymbol{R}^i + \boldsymbol{A}^i \left(\bar{\boldsymbol{R}}^{ip} + \boldsymbol{A}^{ip} \bar{\bar{\boldsymbol{u}}}^{ip} \right) \tag{3.1}$$

where $\boldsymbol{r}^i$ is an arbitrary point on the surface of the rail, $\boldsymbol{R}^i$ is the point on the rail track geometry with respect to the global coordinate system, $\bar{\boldsymbol{R}}^{ip}$ is the point that defines the location between the rail profile coordinate system and the track geometry, $\boldsymbol{A}^{ip}$ is the orientation between the rail profile coordinate system and the track geometry, and $\boldsymbol{u}^{ip}$ defines the point on the rail geometry in the rail frame of reference. Usually, $\boldsymbol{u}^{ip}$ is the point that is defined by the contact surface

curve of the rail surface, which is in turn is a curve swept in the predefined rail geometry. This equation was derived by Shabana (15) to explain the FFR and was used by Rathod et al. (16).

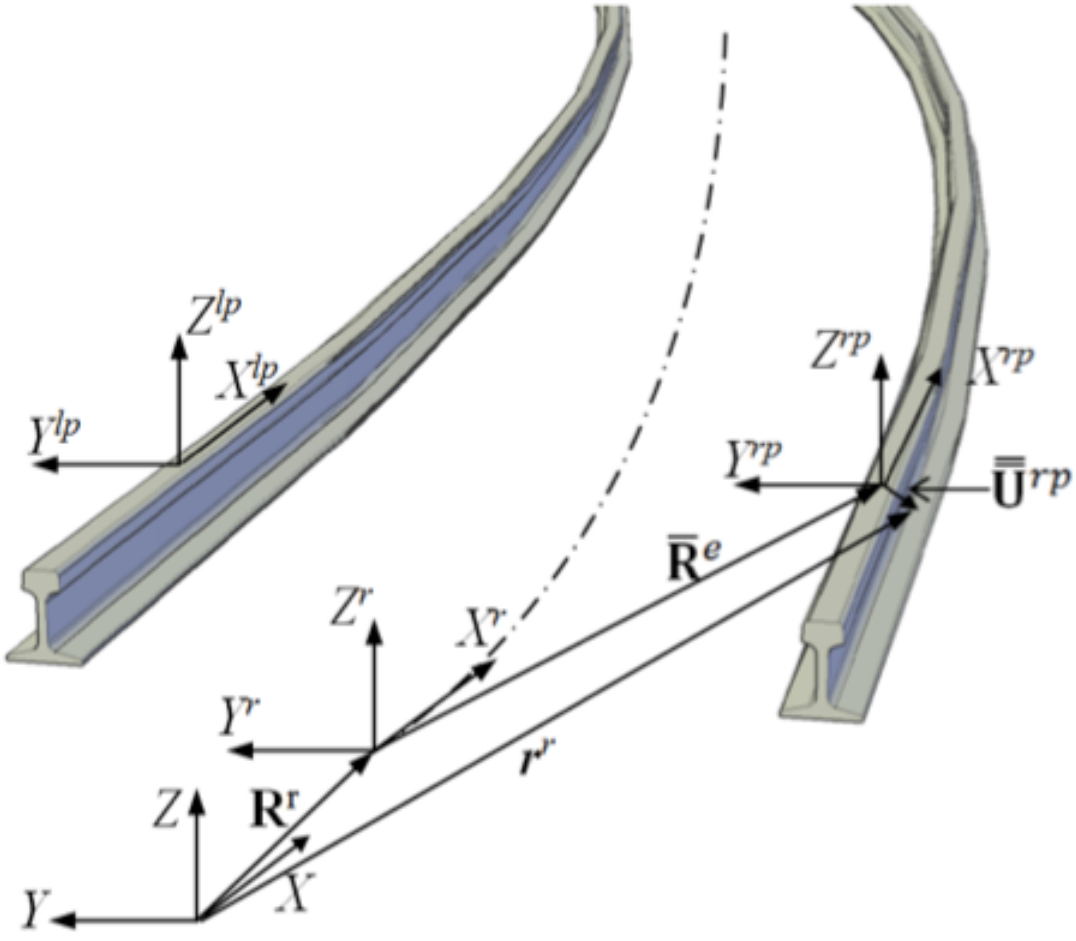

Figure 4. Floating frame of reference for the rail-track geometry

The rail geometry shown in Figure 4 is a result of the modal positioning principal, described in Shabana (15), by the ANCF technique. Any point on the 3D element can be described by the equation

$$\bar{\boldsymbol{R}}^{ip}(x^i, y^i, z^i) = \boldsymbol{S}(x^i, y^i, z^i)\boldsymbol{e}^i(t) \tag{3.2}$$

where $\boldsymbol{S}$ is the shape function matrix of the given element $\boldsymbol{e}^i$ is the vector of time-dependent nodal coordinates and their spatial derivatives of the position of the rail space curve. The coordinates are the local positions on the rail surface geometry. The time-dependent vector $\boldsymbol{e}^i$ should be constantly updated with the deformation of the finite element model.

Using the floating frame of reference, the vector coordinates $\boldsymbol{e}^i$ are updated using the nodal displacements and shape functions. The corresponding nodes of the FE model do not need to coincide with the geometric model of the rail, as shown in Figure 5 and discussed in (15). A point on a finite element of the rail may be described by the equation (15),

$$\bar{\boldsymbol{r}}^{ij} = \boldsymbol{R}^{ij} + \boldsymbol{A}^i \left(\bar{\boldsymbol{u}}_0^{ij} + \bar{\boldsymbol{u}}_f^{ij} \right), \quad j = 1, 2, 3, ..., n_e \tag{3.3}$$

As described in Rathod et al. (16), $\boldsymbol{R}^i$ defines the position of the track coordinate system, $\boldsymbol{A}^i$ is the orientation of the track coordinate with respect to the global coordinates, and n_e is the number of finite elements in the rail model. The vectors $\bar{\boldsymbol{u}}_0^{ij}$ and $\bar{\boldsymbol{u}}_f^{ij}$ are the positions of the point in the reference and current configurations, respectively.

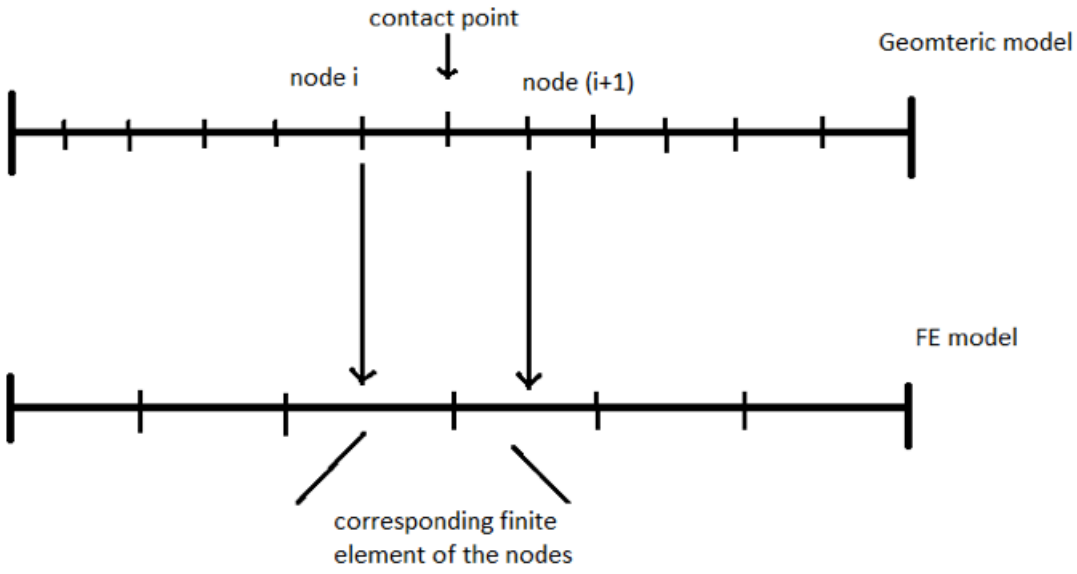

Figure 5. Geometric and FE model of the rail

3.1 Contact formulation

There have been a number of approaches for modeling the contact between two bodies. As discussed by Meli and Pugi (17), a linear superposition principal may be used to approximate the contact point. The elastic contact formulation technique (ECF) by Shabana et al. (8) is discussed in the paper by Meli and Pugi (17). This algorithm does not treat the contact problem as a constraint, but uses a penalty stiffness to approximately enforce the impenetrability between contacting bodies. The parameters of the surface are defined using non-generalized coordinates that define the surface points of the rail/wheel contact. The equation for finding the surface points on the track is

$$\boldsymbol{E}(\boldsymbol{s}) = [\boldsymbol{t}_1^r \cdot \boldsymbol{r}^{wr} \quad \boldsymbol{t}_2^r \cdot \boldsymbol{r}^{wr} \quad \boldsymbol{t}_1^w \cdot \boldsymbol{n}^r \quad \boldsymbol{t}_2^w \cdot \boldsymbol{n}^r]^T = \boldsymbol{0} \tag{3.4}$$

as described by Rathod et al. (16), where $\boldsymbol{E}(\boldsymbol{s})$ is the location of the contact point, $\boldsymbol{t}_i^j$ is the tangent vector on surface j with respect to surface parameter i, $\boldsymbol{r}^{wr}$ is the reference point of the relative position on the rail to the point on the wheel which defines the contact geometry and $\boldsymbol{n}^r$ is the normal to the rail at the point of contact. The contact formulation of the rail-wheel geometry can be classified as a penetration or the separation problem, where the magnitude of the penetration δ is determined by the equation $\delta = \boldsymbol{r}^{wr} \cdot \boldsymbol{n}^r$, where a negative value would suggest penetration and a positive value would suggest a separation between the rail and wheel surface. Penetration proves that there is a contact between the surfaces and therefore the contact forces can be formulated between the rail/wheel contact pair.

For $\delta < 0$, the normal force is computed as $F^N = -K_H\delta^{3/2} - C\dot{\delta}|\delta|$, where K_H is the Hertzian contact constant, C is the damping constant, and $\dot{\delta}$ is the time derivative of the magnitude of the penetration between the rail and the wheel (18). Along with the normal forces, we also get the position and size of the Hertzian contact patch as well as the spin and tangential creepage from the model formulated in Shabana et al. (8), which is based on Kalker's theory (18). The geometry is updated at each time step of the simulation to continuously locate the contact positions and normal forces.

3.2 Simulation of rail-wheel interaction

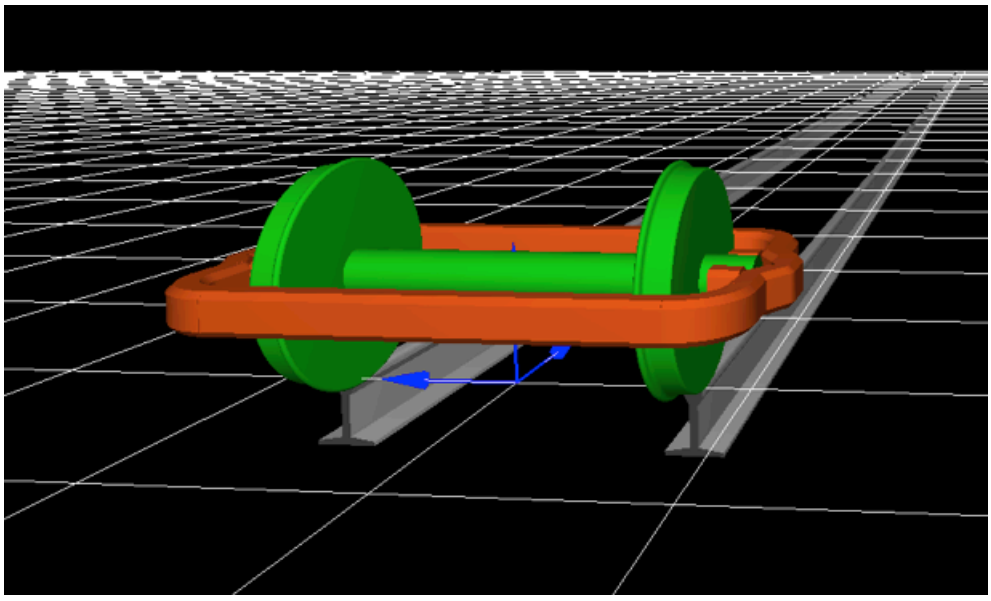

Figure 6. Model of suspended wheels in SAMS

SAMS is a software package which analyses the dynamics between the articulated systems. For our research the input file for SAMS is generated by the PreSAMS file. This software solves the set of differential and algorithmic equations of motion that define the multibody system.

Rail-wheel dynamics is a classic application of multibody analysis. The code uses data from different bodies and simulates the specified interaction between them. Models for wheelsets have already been developed in SAMS, and we couple our data from the finite element as described previously. There are two types of wheelsets that are available for simulation in SAMS. One is the unsuspended wheelset, which is connected to the rail tracks geometrically, and the other one is the suspended wheelset, where the train wheelset can be independently modeled and the geometric nodes could be then set depending on the actual finite element model. We apply the suspended wheelset in this problem. The geometry is shown in Figure 6.

The output file that we extract after running PreSAMS, i.e. the SamsdataT file, is the input file for the suspended wheelset problem. This code uses the nodal coordinates of the FE model created in ANSYS to determine the coordinates of the geometrical nodes on to the wheelset. The model we created on MAPDL had specific rail nodes. Since the stiffness of the substructure is associated to the nodes through the mode shapes, only the nodes of the rail are used in the multibody analysis. The analysis of the rail-wheel interaction is used to extract the contact forces and the time-dependent modal displacements.

3.3 Multibody systems code using SAMS (Simulation of Articulated Mechanical Systems)

Once we have calculated the forces on the rail track, we can calculate the modal forces as discussed by Shabana et al. (8) using SAMS

$$(\boldsymbol{Q}_e)_f = \Psi(\boldsymbol{i})^t \boldsymbol{f} \tag{3.5}$$

where, $(\boldsymbol{Q}_e)_f$ is the modal force, $\Psi(\boldsymbol{i})^t$ is the i^{th} generalized eigenvector extracted from the FE model and $\boldsymbol{f}$ is the nodal applied force. The applied force can be written in the vector form as

$$\boldsymbol{f} = \left\{ \begin{array}{c} \boldsymbol{f}_r \\ \\ \boldsymbol{f}_o \end{array} \right\} \tag{3.6}$$

where, $\boldsymbol{f}_r$ is the force on the nodes that are kept for the multibody simulation (i.e. the nodes on the rail) and $\boldsymbol{f}_o$ is the force on the nodes those were eliminated for the simulation (i.e the nodes not on the rail). In this problem the forces on the nodes not on the rail are zero, and hence the only force considered in $\boldsymbol{f}_r$. Thius, the equation finally becomes

$$(\boldsymbol{Q}_e)_f = \Psi_r(\boldsymbol{i})^t \boldsymbol{f}_f \tag{3.7}$$

where $\Psi_r(\boldsymbol{i})$ represents the truncated eigenvectors.

Ebrahimi et al. (19) have discussed the multibody dynamics of contact problems. Multibody dynamics has its foundation from the various analytical and numerical methodologies

of simulating complex mechanical systems. With the advent of more computational power, multibody dynamics has attracted more attention as a powerful tool for analyzing mechanical systems. With better computational power available, we have been successfully able to couple our FE model with multibody dynamics code. G Kumaran et al. (2) has discussed in his study regarding the various methods of modeling contact in rail-wheel interaction. This discussion includes how the model takes into account the effects of the dynamics of the rail-wheel interaction on the basis of the vehicle dynamics and how the forces are exerted on the tracks. The other module is the track model which takes into account the properties of the tracks on the sleepers and substructure. The interaction between the track and vehicle is then carried out in the time domain using transient analysis option in the multibody code. For multibody dynamics part of the study, the software we used was SAMS (Simulation of Articulated Mechanical Systems).

The wheel exerts a time-dependent force of the rail. The extraction of those transient forces is done on the multibody dynamics software. The modal displacements are also solved. The SAMS run produces results through which we are able to quantify the motion of the rail.

3.3.1 Equations of motion

In this research, we have used the augmented formulation of multibody equations, as detailed in Shabana et al. (8). The augmented method of motion uses Lagrange multipliers to define system constraints and extract the motion. The augmented equation is defined as

$$\begin{bmatrix} \boldsymbol{m}_{rr} & \boldsymbol{m}_{rf} \\ \boldsymbol{m}_{fr} & \boldsymbol{m}_{ff} \end{bmatrix} \begin{bmatrix} \ddot{\boldsymbol{q}}_r \\ \ddot{\boldsymbol{q}}_f \end{bmatrix} = \begin{bmatrix} (\boldsymbol{Q}_e)_r \\ (\boldsymbol{Q}_e)_f \end{bmatrix} + \begin{bmatrix} (\boldsymbol{Q}_v)_r \\ (\boldsymbol{Q}_v)_f \end{bmatrix} - \begin{bmatrix} \boldsymbol{C}_{qr}^T \\ \boldsymbol{C}_{qf}^T \end{bmatrix} \boldsymbol{\lambda} - \begin{bmatrix} \mathbf{0} \\ \boldsymbol{K}_{ff}\boldsymbol{q}_f \end{bmatrix} \tag{3.8}$$

where $\boldsymbol{m}_{rr}$ is the inertia matrix for the reference coordinates, $\boldsymbol{m}_{rf}$ and $\boldsymbol{m}_{fr}$ are the inertia matrices for the coupling of the elastic and reference coordinate systems, $\boldsymbol{q}_f$ is the vector of the elastic modal coordinates and $\boldsymbol{q}_r$ is the vector of the generalized coordinates in the floating frame of reference. These equations define the motion of the structure. The vectors $(\boldsymbol{Q}_e)_r$ and $(\boldsymbol{Q}_e)_f$ are vectors of the generalized external forces for the rigid and elastic coordinates, respectively. $(\boldsymbol{Q}_v)_r$ and $(\boldsymbol{Q}_v)_f$ are the vectors of velocity inertia forces related to the rigid and elastic coordinates respectively, $\boldsymbol{C}_{qr}^T$ and $\boldsymbol{C}_{qf}^T$ are the Jacobian matrices arising from the constraint equations for the rigid and elastic coordinates, $\boldsymbol{\lambda}$ is a vector of Lagrange multipliers, and $\boldsymbol{K}_{ff}$ is the stiffness matrix for the track. The augmented formulation, as discussed by Shabana (15), results in a set of differential and algebraic equations with Lagrange multipliers that are solved simultaneously. The multibody system that is being studied can be solved for reference and elastic accelerations using a sparse matrix solver. As discussed by Shampine et al. (20), time integration is performed using the Adams-Bashforth technique.

CHAPTER 4

RECONSTRUCTION OF RESULTS

The simulation done on SAMS (Simulation of Articulated and Mechanical System) solves for the time-dependent modal displacements of the rail and substructure. As discussed by Shabana et al. (8), the nodal displacements can be determined from the equation

$$\boldsymbol{U}_f = \boldsymbol{S}\boldsymbol{q}_f \tag{4.1}$$

where $\boldsymbol{U}_f$ is the nodal displacement vector the body, $\boldsymbol{S}$ is the mode shape matrix of the vibrating structure and $\boldsymbol{q}_f$ is the vector of modal displacements of the structure which was extracted from the MBS code. The nodal displacements are extracted using a MATLAB code that reconstructs the nodal displacement from the modal displacements determined from the multibody simulation.

In previous research (12), the mode shapes have been used to create an efficient model of the track substructure. However, in that research, the substructure model was developed to understand its effect on rail-wheel interaction, and the response of the substructure itself was never fully analyzed. In this work, we use the modal displacements to reconstruct the full response of the track substructure. After displacements are reconstructed, other quantities such as velocity, acceleration, and strain can be determined. In particular, we are interested in the accelerations at the building.

CHAPTER 5

NUMERICAL EXAMPLE

The example used in this research is a 3D model of railroad comprising of railroad, fasteners, sleepers, and substructure. The numerical model is similar to the example discussed by El-Ghandour et al. (12) in his paper. The schematic diagram showing all the layers is shown in Figure 7. In three dimensions, we extend the subgrade layer horizontally to the foundation of the building.

5.1 Simulation of rail-wheel interaction

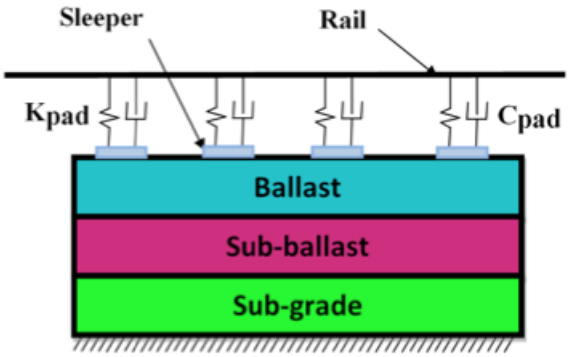

Figure 7. Schematic diagram of the finite element model showing the layers of the substructure. K_{pad} and C_{pad} are the stiffness and damping, respectively, arising from the fastener and pad assembly.

The material properties are shown in Table 1. These properties are similar to those used in (12).

Description	Value	units
Rigid rail length	18 (on each side)	m
Gauge length	1.5113	m
Rail stiffness (E_r)	210e9	N/m^2
Rail density (ρ_r)	7700	kg/m^3
Rail Poisson's ratio (ν_r)	0.3	
Rail cross section area (A_r)	64.5e-4	m^2
Rail area moment of inertia (I_{yy})	2010e-8	m^4
Rail area moment of inertia (I_{zz})	326e-8	m^4
Rail Timoshenko shear coefficient	0.34	
Sleeper length	2.36	m
Gap between sleepers	0.65	m
Sleeper Young's modulus (E_s)	64e9	N/m^2
Sleeper density (ρ_s)	2700	kg/m^3
Sleeper Poisson's ratio (ν_s)	0.33	
Sleeper cross section area (A_r)	513.8e-4	m^2
Sleeper area moment of inertia (I_{yy})	18907e-8	m^4
Sleeper Timoshenko shear coefficient	0.83	
Pad stiffness coefficient (K_{pad})	26.5e7	N/m
Pad damping coefficient (C_{pad})	2.0e5	Ns/m
Ballast Young's modulus (E_b)	260e6	N/m^2
Ballast density (ρ_b)	1250	kg/m^3
Ballast Poisson's ratio (ν_b)	0.3	
Subballast Young's modulus (E_{sb})	200e6	N/m^2
Subballast density (ρ_{sb})	1850	kg/m^3
Subballast Poisson's ratio (ρ_{sb})	0.33	
Subgrade Young's modulus (E_{sg})	200e6	N/m^2
Subgrade density (ρ_{sg})	1850	kg/m^3
Subgrade Poisson's ratio (ρ_{sg})	0.33	

TABLE I

MATERIAL PROPERTIES FOR THE RAIL AND BUILDING MODEL

5.2 Contact forces

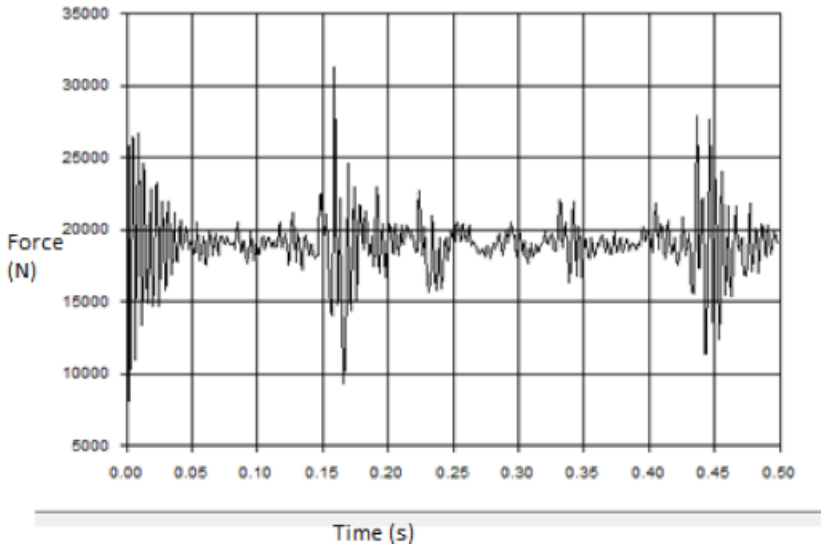

Figure 8. Contact forces on the rail due to the passing wheelset.

Figure 8 shows the contact forces during the rail-wheel interaction. These forces were generated directly in the SAMS simulation. They are similar in magnitude to those seen in El-Ghandour et al. (12).

5.3 Displacement and strain in the substructure

Figure 9 shows the reconstruction of the deformation of the structure at one of the time step. Here, in the nodal solution plot of the displaced structure shows us the effects of forces on the rail substructure. When the wheel moves over the tracks, weight of the train causes

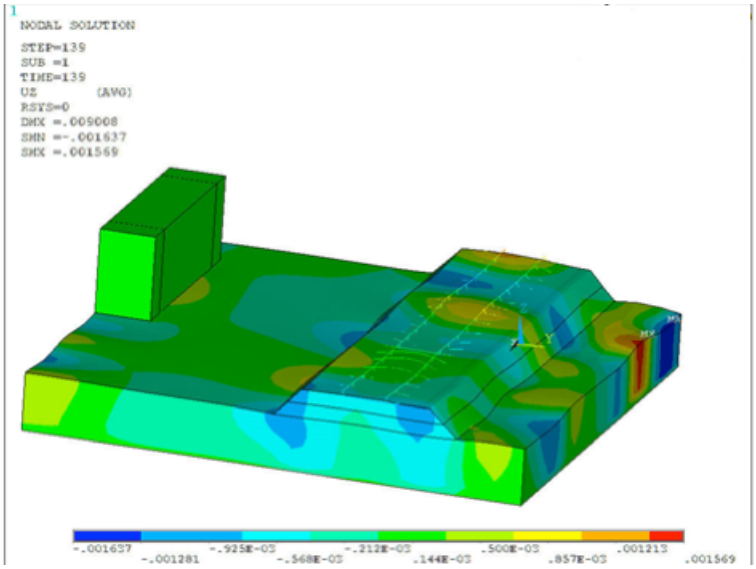

Figure 9. Deformed shape of the substructure 3/4 through the simulation, colored by vertical displacement.

vibrations to pass through the soil. Some of the vibrations are absorbed by the rail pads and sub-structure. The building structure has a relatively small deformation compared to the rail as most of the loading due the wheel movement is absorbed by the rail sub-structure. However, in this example, the vibration is still strong enough to reach the building and cause occupant discomfort.

Figure 10 shows the equivalent strain of the railroad structure. While not the focus of this study, it is interesting to see other quantities that can be visualized from reconstructing the displacements. The strain is highest in the subgrade near the edge of the ballast and subballast layers. Here there is more shear, and the softer subgrade is more susceptible to strain. There is also some concentration of strain due to edge effects of the simulation.

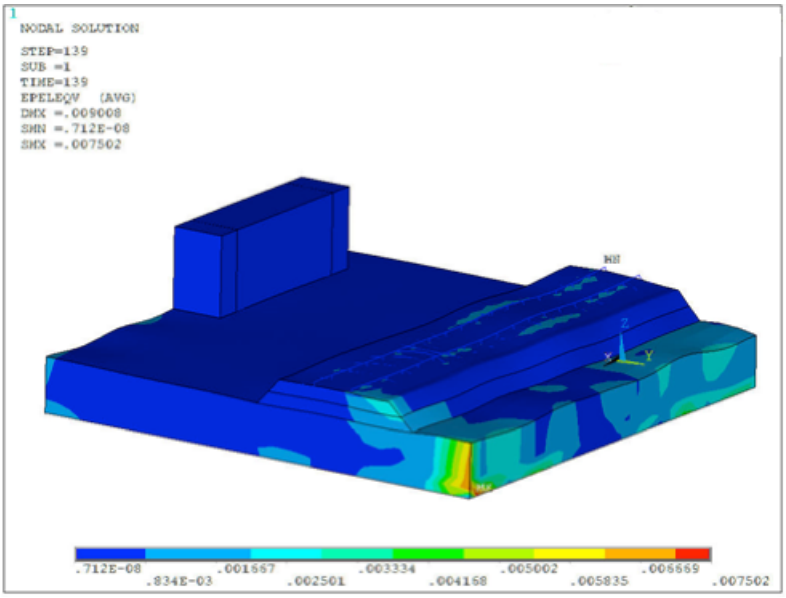

Figure 10. Equivalent strain in the in the substructure 3/4 of the way through the simulation.

5.4 Displacement over time

Figure 11 shows the plot of the normal displacement in the lateral direction at a node near the base of the building. This plot can be reconstructed using ANSYS software. The magnitude of the vibrations increases as the wheelset passes closer to each building.

5.5 Vibration quantification

The nodal accelerations may be reconstructed in the same manner as the displacements. In terms of occupant comfort and structural damage, acceleration is generally the most important component. We sample the vibrations on various nodes on the structure to see where the accelerations would be highest. Considering the proximity of the structure to the railroad, the

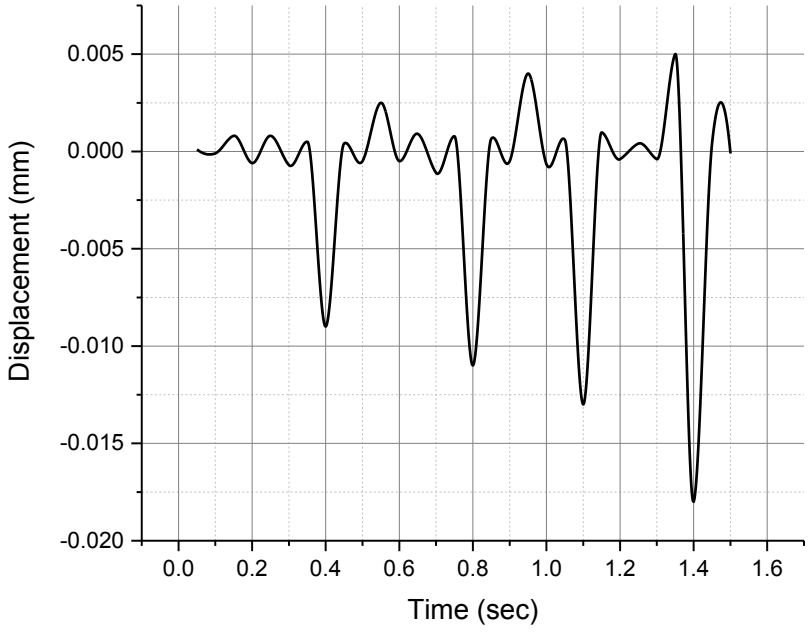

Figure 11. Displacement-time plot of a point on the base of the structure.

magnitude of vibrations on the building were realistic. Proximity is the most important factor in quantifying the vibrations, but material properties and geometry are also important.

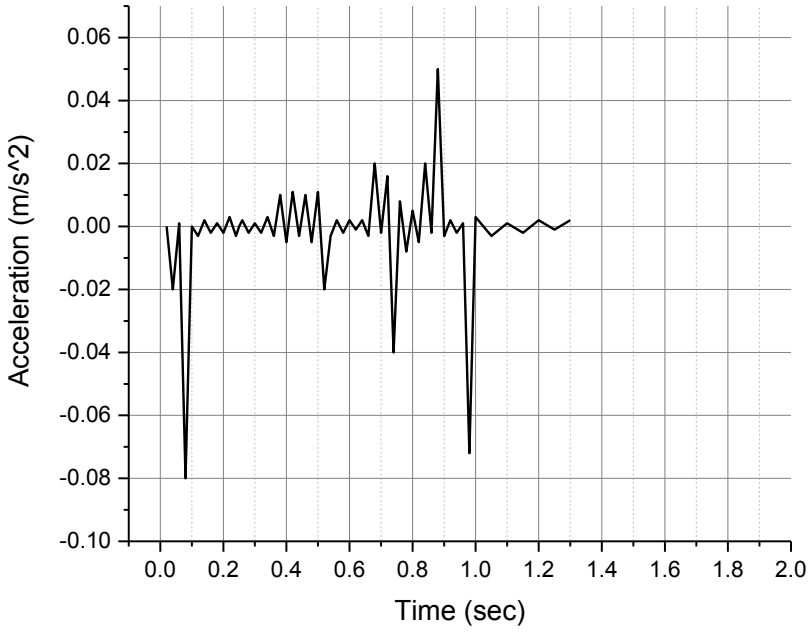

Figure 12. Acceleration of a node near the top of the structure

Figure 12 shows the displacement of node 4263, which is one of the top most nodes of the building structure. The plot shows the deformation due to the wheel movement on the rail tracks. Extracting the accelerations dependent on the deformations of the nodes, we were

able to quantify the vibrations on the building. Bednarz and Targosz (6) suggested that if the acceleration amplitude exceeds 0.005g, there would some unpleasant experience for the occupants. Murray et al. (21) developed a comfort criteria based on vibrations felt in the building. Depending on the nature of vibrations, vibrations from 0.5% to 5% of the acceleration due to gravity could cause occupant discomfort. Based on the plot we have, the acceleration does exceeds those values, indicating some occupant discomfort is likely. Apart from the acceleration of the top of the building, the acceleration at the mid node and the one on the bottom part of the building were plotted.

Figure 13 shows the vibration acceleration amplitude at node 1047, which is one of the middle nodes on the building. As we can see, the accelerations here are a little higher than on the top most node of the building.

Figure 14 shows the accelerations amplitude plot for the node that is at the base of the building. The accelerations felt here are relatively higher than at the other nodes. The accelerations are in a descending order with the maximum vibrations felt at the bottom, gradually decreasing towards the top. For shorter buildings such as this one, the the accelerations will be stronger at the base, and the areas farther up will be see reduced vibrations. Taller buildings may see larger displacements at the top as the building bends.

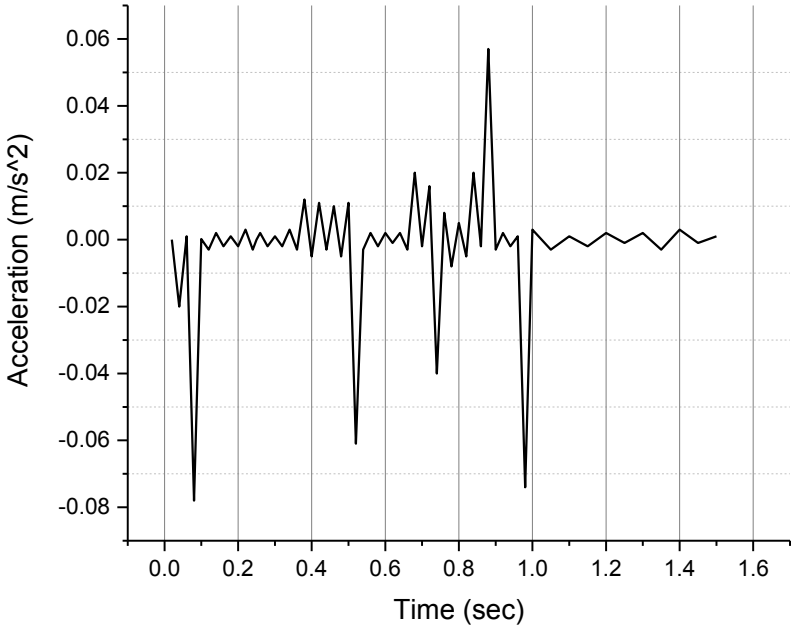

Figure 13. Acceleration of a node near the middle of the structure

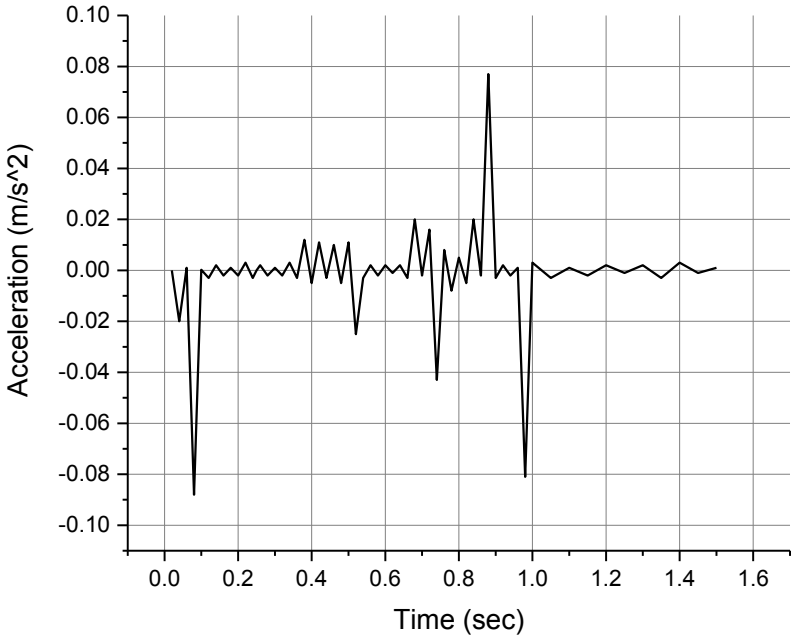

Figure 14. Acceleration of a node near the bottom of the structure

CHAPTER 6

CONCLUSIONS AND FUTURE WORK

6.1 Conclusions

A 3D finite element model of a railway with substructure was created in ANSYS with rails, sleepers, ballast, soil, and a building model for the purpose of examining vibrations caused by passing trains. The rail and sleepers were modeled with beam elements, whereas ballast, sub-ballast, and sub-grade were modeled using three-dimensional brick elements. Spring-damper elements were used for the rail pads and fasteners. We extracted the modal mass and stiffness values of the finite element model and input this information into a multibody code to simulate the passing of a suspended wheelset. The MBS code calculated the contact forces of the rail-wheel interaction during the simulation as well as the resulting modal deformations. We were then able to reconstruct the nodal deformations of the substructure and input this information into ANSYS to post-process and visualize the results. We used these deformations to quantify the accelerations on the building in our model. By understanding the vibrations in the building, occupant discomfort could be evaluated. Examining the accelerations at different points on the building, we can conclude that the amplitude differs at different points in the structure. In this example, there is enough acceleration to create occupant discomfort. For a shorter building such as this, accelerations are higher at the base of the building where they are exposed to soil

vibrations. For taller structures, flexibility may lead to stronger motion in the upper part of the building.

6.2 Future work

This model can be applied to real scenarios to evaluate vibrations in the structures constructed near the railroad, though more field validation is necessary to ensure the results are accurate. The formulation can also be used to understand and investigate vibration mitigation techniques, from different railpad designs to different materials that can be used in making fasteners, to damping materials in the sub-structure.

A more sophisticated railroad model with a visco-plastic material model for the soil is also planned in the future. The geometric model of the railroad structure would remain the same with only the material attributes changing adding a more realistic damping model. The reconstruction of the deformations of the sub-structure can be used to study soil settlement and other issues in rail sub-structure.

APPENDICES

Appendix A

SAMS INPUT FILE

The input file used in SAMS for the rail-wheel interaction simulation is called the SAMS-data.dat, which includes the rail module properties like the coordinates of the rail nodes, the length of the rail and the distance between them. It also includes the speed of the train. Figure 15, Figure 16, and Figure 17 show the input file which is used to extract the contact forces for the rail-wheel interaction. The SAMS file details the rail model in the MBS code.

Appendix A (Continued)

```
SAMS-Mode
 0
=====================================================================
===============
SuspendedWheelset
=====================================================================
===============
 3
Spatial-Analysis
=====================================================================
===============
 131
Number-of-the-System-Degrees-of-Freedom
=====================================================================
===============
 2              0              0              0              1000000
1              0              50001          0              0
0              0              0
 0
Initialization-Parameters
=====================================================================
===============
 6              3
Number-of-Bodies
 Masses-and-mass-moments-of-inertia-of-the-bodies
Rail
 1              0              0              0              0
0              0              0
Wheelset
 2              1568           656            168            656
0              0              0
Frame
 3              10000          1799           1799           2450
0              0              0
```

Figure 15. Part 1 of the SAMS input file.

Appendix A (Continued)

```
SAMS-Mode
 0
=====================================================================
===============
SuspendedWheelset
=====================================================================
===============
 3
Spatial-Analysis
=====================================================================
===============
 131
Number-of-the-System-Degrees-of-Freedom
=====================================================================
===============
 2              0              0              0              1000000
1              0              50001          0              0
0              0              0
 0
Initialization-Parameters
=====================================================================
===============
 6              3
Number-of-Bodies
 Masses-and-mass-moments-of-inertia-of-the-bodies
Rail
 1              0              0              0              0
0              0              0
Wheelset
 2              1568           656            168            656
0              0              0
Frame
 3              10000          1799           1799           2450
0              0              0
```

Figure 16. Part 2 of the SAMS input file.

Appendix A (Continued)

```
SAMS-Mode
 0
================================================================
===============
SuspendedWheelset
================================================================
===============
 3
Spatial-Analysis
================================================================
===============
 131
Number-of-the-System-Degrees-of-Freedom
================================================================
===============
 2              0              0              0              1000000
1              0              50001          0              0
0              0              0
 0
Initialization-Parameters
================================================================
===============
 6              3
Number-of-Bodies
 Masses-and-mass-moments-of-inertia-of-the-bodies
Rail
 1              0              0              0              0
0              0              0
Wheelset
 2              1568           656            168            656
0              0              0
Frame
 3              10000          1799           1799           2450
0              0              0
```

Figure 17. Part 3 of the SAMS input file.

CITED LITERATURE

1. Engineering, A. R. and of Way Association, M.: Manual for railway engineering. Lanahm, MD, American Railway Engineering and Maintenance-of-Way Association, 2015.

2. Kumaran, G., Menon, D., and Nair, K.: Dynamic studies of railtrack sleepers in a track structure system. Journal of Sound and Vibration, 268(3):485–501, Nov 27 2003.

3. Sladkowski, A. and Sitarz, M.: Analysis of wheel-rail interaction using FE software. Wear, 258(7-8):1217–1223, MAR 2005. 6th International Conference on Contact Mechanics and Wear of Rail/Wheel Systems, Gothenburg, Sweden, Jun 10-13, 2003.

4. Monfared, V.: Contact stress analysis in rolling bodies by finite element method (fem) statically. 2012.

5. Li, M. X., Ekevid, T., and Wiberg, N.-E.: Modelling of railway vehicle-track-underground dynamic interaction induced by high-speed trains. 2003.

6. Bednarz, J. and Targosz, J.: Finite elements method in analysis of vibrations wave propagation in the soil. Journal of KONES Powertrain and transport, 18(3), 2011.

7. Verbraken, H., Eysermans, H., Dechief, E., François, S., Degrande, G., and Lombaert, G.: Development of a hybrid prediction method for railway in-duced vibration.

8. Shabana A. A., Zaazaa K. E., . S. H.: Railroad vehicle dyanmics: A computational approach. Boca Raton, FL, Taylor and Francis/CRC, 2007.

9. Recuero A. M., Escalona J. L., . S. A. A.: Finite-element analysis of unsupported sleepers using three-dimensional wheelrail contact formulation. Proceedings of the Institution of Mechanical Engineers, Part K: Journal of Multi-body Dynamics, 225(2):153–165, 2011.

10. Tanabe, M., Wakui, H., Sogabe, M., Matsumoto, N., and Tanabe, Y.: A combined multi-body and finite element approach for dynamic interaction analysis of high-speed train and railway structure including post-derailment behavior during an earthquake. IOP Conference Series: Materials Science and Engineering, 10(1):012144, 2010.

11. Galvín, P., Romero, A., and Domínguez, J.: Fully three-dimensional analysis of high-speed train–track–soil-structure dynamic interaction. Journal of Sound and Vibration, 329(24):5147–5163, 2010.

12. El-Ghandour, A. I., Hamper, M. B., and Foster, C. D.: Coupled finite element and multibody system dynamics modeling of a three-dimensional railroad system. Proceedings of the Institution of Mechanical Engineers, Part F: Journal of Rail and Rapid Transit, page 0954409714539942, 2014.

13. Vlasenko, D. and Kasper, R.: Generation of equations of motion in reference frame formulation for fem models. Engineering Letters, 16(4):537–544, 2008.

14. Shabana, A. A. and Yakoub, R. Y.: Three dimensional absolute nodal coordinate formulation for beam elements: theory. Journal of Mechanical Design, 123(4):606–613, 2001.

15. Shabana, A.: Dynamics of Multibody Systems. Cambridge, Cambridge University Press, 2005.

16. Rathod, C., Chamorro, R., Escalona, J., El-Sibaie, M., and Shabana, A.: Validation of three-dimensional multi-body system approach for modelling track flexibility. Proceedings of the Institution of Mechanical Engineers, Part K: Journal of Multi-body Dynamics, 223(4):269–282, 2009.

17. Meli, E. and Pugi, L.: Preliminary development, simulation and validation of a weigh in motion system for railway vehicles. Meccanica, 48(10):2541–2565, 2013.

18. Kalker, J. J.: Three-dimensional elastic bodies in rolling contact, volume 2. Springer Science & Business Media, 2013.

19. Ebrahimi, S. and Eberhard, P.: Aspects of contact problems in computational multibody dynamics. In Multibody Dynamics, pages 23–47. Springer, 2007.

20. Shampine, L. F. and Gordon, M. K.: Computer solution of ordinary differential equations: the initial value problem. WH Freeman San Francisco, 1975.

21. Murray, T. M., Allen, D. E., and Ungar, E. E.: Floor vibrations due to human activity. American Institute of Steel Construction, 2003.

22. Ulker-Kaustell, M.: Some Aspects of the Dynamic Soil-Structure Interaction of the Porter Frame Railway Bridge. Doctoral dissertation, Licentiate thesis, 2009.

23. Kaewunruen, S. and Remennikov, A.: Nonlinear finite element modelling of railway prestressed concrete sleeper. Faculty of Engineering-Papers, page 319, 2006.

24. Uzzal, R. U. A., Ahmed, W., and Rakheja, S.: Dynamic analysis of railway vehicle-track interactions due to wheel flat with a pitch-plane vehicle model. Journal of Mechanical Engineering, 39(2):86–94, 2008.

25. Zania, V., Hededal, O., and Krogsbøll, A.: Train induced vibrations in geosynthetic reinforced railway embankments. In 8th International Conference on Structural Dynamics, EURODYN, pages 692–698, 2011.

26. Pal, B., Dey, K., and Tandia, P. K.: Vibrations on structures and soils due to industrial activities: unique case studies and mitigation measures. Journal of Environmental Research And Development Vol, 4(3), 2010.

27. Al Suhairy, S.: Prediction of ground vibration from railways. Swedish National Testing and Research Institute, 2000.

28. Chen, P.-w.: Vibration of nearby structures induced by High-speed rail transit. ProQuest, 2008.

29. Dietz, S., Wallrapp, O., and Wiedemann, S.: Nodal vs. modal representation in flexible multibody system dynamics. Proceedings of multibody dynamics, pages 1–4, 2003.

30. Rathod, C. and Shabana, A. A.: Geometry and differentiability requirements in multibody railroad vehicle dynamic formulations. Nonlinear Dynamics, 47(1-3):249–261, 2007.

VITA

Chaitanya R Joshi
Email: cjoshi4@uic.edu
www.linkedin.com/in/chaitanyajoshi1

EDUCATION

University of Illinois at Chicago: **Graduation Expected: January 2016**
Master of Science in Mechanical engineering (GPA: 3.67)

University of Mumbai: **August 2013**
Pursued Bachelors' in mechanical engineering (GPA: 3.5)

Relevant Courses:
Finite element analysis, Advanced finite elements, Dynamics of multibody systems, Continuum mechanics, applied stress analysis, advanced Fluid dynamics, Heat and mass transfer, Computer Aided Design (CAD), advanced Design.

WORK EXPERIENCE

Testing engineer co-op at ANSYS Inc. **May 2015-September 2015**

- Working as a testing engineer co-op in the MAPDL development team in the non-linear procedures division.
- Responsibilities include testing the input cases for clients on non-linear adaptivity feature for 2D and 3D dynamic problems.
- Also worked on composites and reinforced element feature in Workbench and MAPDL.
- Have been successfully tested the non-linear contact feature for the most recent MAPDL version with structural and thermal modules on ANSYS Multiphysics and Workbench.
- Have successfully tested over 40 non-linear contact problems on windows as well as linux machines
- More recently have implemented a few test cases for the new features of MAPDL on Workbench as well.

RESEARCH

Graduate researcher at Dynamic Simulations Lab: **March 2014 – May 2015**.

- Working on railroad dynamics and 3D non-linear FEA modelling which is the topic for my research thesis as well.
- Using the fundamentals of continuum mechanics, computational dynamics and non-linear FEA, presently studying the effects of the vibrations of the wheel assembly on the fastener system of the rail track.
- Developed a 3D railroad model on ANSYS and currently simulating the effects of contact forces on SAMS.
- Successfully simulated the effects of structural and mechanical vibrations on MATLAB with an error less than 5%.
- Currently working on the discretization of the contact between the sleeper and the wheel to understand the elemental changes of the structure.

PROJECTS

- **Condition based monitoring and thermal flow analysis of a hydrodynamic journal bearing**:
  Transient thermal flow analysis using monitoring and simulating techniques was performed on hydrodynamic journal bearing. Implemented the pressure and temperature distribution using the fluid flow analysis.
- **Design and manufacturing of the chassis of an All-Terrain Vehicle**:
  Designed the ATV chassis and the steering system on Catia V5 and analysed the vehicle's exhaust and engine's fluid and heat flow on ANSYS workbench. The design was made using DFA and DMA principles.
- **Dynamic analysis of a fluid flowing through a porous medium:**
  Performed a transient fluid flow analysis through a porous medium using the concepts of 'POROMECHANICS' and advanced finite element modelling on Matlab.

CERTIFICATION

- ANSYS certification for advanced non-linear contacts on Workbench.
- ANSYS certification for advanced material modelling and composites testing.

COMPUTER SOFTWARE SKILLS

- ANSYS, Solidworks, C++, Catia V5, Creo 2.0, Matlab, Simulink, AutoCAD, Nastran, Comsol, Microsoft office.